

## The Membrane Potential of Ehrlich Ascites Tumor Cells Microelectrode Measurements and Their Critical Evaluation

U. V. LASSEN, A.-M. T. NIELSEN, L. PAPE, and L. O. SIMONSEN

Zoophysiological Laboratory B, August Krogh Institute,  
University of Copenhagen, Copenhagen, Denmark

Received 30 March 1971

*Summary.* Intracellular potentials were measured, using a piezoelectric electro-mechanical transducer to impale Ehrlich ascites tumor cells with capillary microelectrodes. In sodium Ringer's, the potential immediately after the penetration was  $-24 \pm 7$  mV, and decayed to a stable value of about  $-8$  mV within a few msec. The peak potentials disappeared in potassium Ringer's and reappeared immediately after resuspension in sodium Ringer's, whereas the stable potentials were only slightly influenced by the change of medium. The peak potential is in good agreement with the Nernst potential for chloride. This is also the case when cell sodium and potassium have been changed by addition of ouabain. It is concluded that the peak potentials represent the membrane potential of the unperturbed cell, and that chloride is in electrochemical equilibrium across the cell membrane.

The membrane potential of about  $-11$  mV previously reported corresponds to the stable potential in this study, and is considered as a junction potential between damaged cells and their environment. Similar potential differences were recorded between a homogenate of cells and Ringer's.

The apparent membrane resistance of Ehrlich cells was about  $70 \Omega\text{cm}^2$ . This is two orders of magnitude less than the value calculated from  $^{36}\text{Cl}$  fluxes, and may, in part, represent a leak in the cell membrane.

For comparison, the influence of an eventual leak on measurements in red cells and mitochondria is discussed.

Several studies concerning the membrane potential of Ehrlich ascites tumor cells have been published in the past [1, 3, 9, 13, 21]. The most frequently reported value for the membrane potential is about  $-11$  mV, the inside of the cell membrane being negative with respect to the external fluid. This rather low membrane potential is surprising, as it is less than half the value of the equilibrium potential ( $E$ ) for chloride obtained from the Nernst equation:

$$E = (RT/zF) \ln a_0/a_i = (RT/zF) \ln f_0 c_0/f_i c_i \quad (1)$$

where  $R$  is the gas constant,  $T$  is the absolute temperature,  $z$  is the valency of the ion, and  $F$  is Faraday's number. " $a$ " is the ion activity,  $f$  the activity coefficient and  $c$  the molar concentration of the ion. The subscripts  $i$  and  $0$  refer to the intracellular and extracellular phases. In the calculation of the Nernst potential, any contribution from a non-exchangeable fraction of cell chloride is neglected since Simonsen and Nielsen [23] have demonstrated the apparent non-exchangeable chloride to be caused by protein interference with the argentimetric titration of chloride.

The above-mentioned discrepancy between the measured membrane potential and the calculated Nernst potential for chloride would indicate that chloride is not in equilibrium across the cell membrane. Either chloride is actively transported or the common assumption of equal activity coefficients for chloride in extracellular and intracellular water is not justified in these cells. A third possibility is that one or more of the involved parameters is incorrectly measured.

The membrane potential is of importance not only for considerations concerning the distribution of chloride ions, but also for the distinction between active and passive transport of other ions across the cell membrane. Therefore, the magnitude of the membrane potential was re-estimated using a modification of the technique of Lassen and Sten-Knudsen [15] for introduction of micropipettes into small cells in suspension. Two magnitudes of potentials were observed: stable values in the order of 8 mV (inside negative), and transient potentials which decayed in a few msec from their initial value of 20 to 25 mV (inside negative) to the stable potential level of about 8 mV. For reasons to be demonstrated below, the stable recordings are considered to represent a junction (diffusion) potential between the extracellular fluid and the content of damaged cells, whereas the transient potentials presumably are close to the "true" membrane potential. The membrane potential thus measured equals the calculated equilibrium potential for chloride.<sup>1</sup>

### Materials and Methods

The cells used in this study were hyperdiploid Ehrlich ascites tumor cells maintained by weekly transplantation into the peritoneum of female NMRI mice weighing 18 to 23 grams. The cells were harvested 6 to 8 days after the transplantation in ice-cold phosphate Ringer's (see Table 1), containing heparin (2 IU/ml). The cells were washed and incubated at 37 °C in Ringer's solution at a cytocrit of 5 to 10%. Tritiated methoxy-inulin (New England Nuclear Corp., Boston, Mass.) as extracellular marker and in many cases <sup>36</sup>Cl (Danish Atomic Energy Commission, Risø, Denmark) was added.

<sup>1</sup> Part of the experimental data was presented at the Third International Biophysics Congress (Cambridge, Mass., 1969).

Table 1. *Compositions of the Ringer's solutions used for washing and incubation of the cells*

Ion species	Sodium Ringer's (mM)	Potassium Ringer's (mM)
Na <sup>+</sup>	148	—
K <sup>+</sup>	5.2	155
Cl <sup>-</sup>	151	153
Ca <sup>++</sup>	1.7	1.7
Mg <sup>++</sup>	1.2	1.2
SO <sub>4</sub> <sup>-</sup>	1.2	1.2
Orthophosphate	3.0	3.0

The pH of the solutions was adjusted to 7.4.

Samples of 500  $\mu$ liter of cell suspension were centrifuged for 30 sec at 18,000  $\times g$  in a centrifuge accelerating to the full rpm in less than 3 sec. The supernatant was removed and precipitated with perchloric acid (PCA) (final concentration, 7%). The pellet of cells was then lysed in 10 volumes of water under careful agitation and precipitated with PCA to a final concentration of 7%. Trapped medium in the cell pellet was determined from the amount of <sup>3</sup>H-inulin in these samples and in the PCA precipitated medium.

Radioactive isotopes (<sup>3</sup>H and <sup>36</sup>Cl) were determined by liquid scintillation counting using a standard toluene-ethanol based scintillation fluid. All samples were counted to a statistical error of less than 1%. Sodium and potassium were determined in an Eppendorf flame photometer (Netheler & Hinz, Hamburg, Germany) employing a propane-air mixture. Chloride was determined by automatic potentiometric titration of the deproteinized samples with AgNO<sub>3</sub>. The reproducibility of the overall procedure for the determination of cellular ion concentrations was better than 5%. (For details of the experimental procedure, *see* ref. [23].)

The influx of <sup>36</sup>Cl into the cells was followed with time, and the rate constant of cellular chloride exchange determined as described by Simonsen and Nielsen [23].

### *Microelectrode Measurements*

To measure the intracellular potential of the ascites cells, a technique essentially similar to the one used for studies on human red cells by Lassen and Sten-Knudsen [15] was employed. For the understanding of the recordings to be presented, the general principle is shown in Fig. 1 together with modifications necessary for the present purpose. Cells in suspension were injected into the perspex covered experimental chamber and allowed to sediment on the bottom, where they could be seen in the field of an inverted microscope. The objective was a Zeiss phase-contrast Neofluar (63  $\times$ , NA 1.30) with a long working distance (0.17 mm). The temperature of the contents of the chamber was held at 37  $\pm$  0.5  $^{\circ}$ C by means of a servo-controlled electric heating system for the objective. Fine movement of the microelectrode mounted on a piezoelectric driver was performed with a Leitz micromanipulator. The piezoelectric electro-mechanical driver was redesigned from the original [15]. In this version, the piezoelectric bender elements were arranged in two parallel rows with 10 elements in each row, one above and one below the movable perspex rod carrying the microelectrode holder. This design gave a doubling of the velocity of advancement of the electrode, a total electrical shielding of the electrode towards

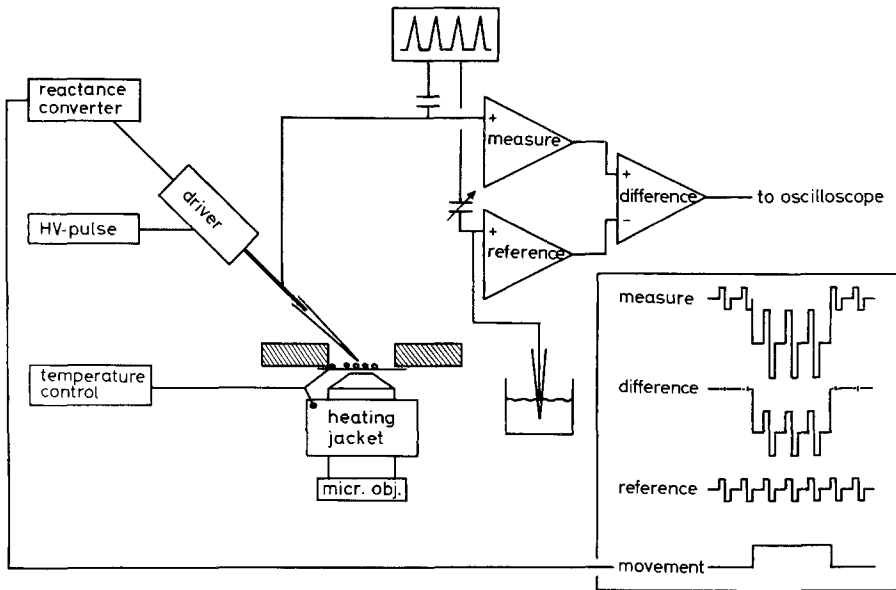


Fig. 1. Simplified diagram of experimental apparatus. The cells in the chamber above the objective of the inverted microscope (micr. obj.) are kept at constant temperature via sensors in the chamber and a servo-controlled heating jacket around the objective. The heat is conducted to the chamber via immersion oil between objective and chamber. The microelectrode is driven into the cell by means of a piezoelectric electro-mechanical transducer (driver) activated by a high-voltage pulse across the piezoelectric elements (HV-pulse). The axial movements of the electrode are monitored by a capacitance transducer and a reactance converter. The potential of the microelectrode is recorded by means of a negative-capacitance amplifier (measure) and fed to the positive input of a difference amplifier. Another microelectrode in a reference bath separate from the measuring chamber is connected to the input of another negative-capacitance amplifier (reference), the output of which is led to the negative input of the difference amplifier. Diphasic constant-current pulses through the microelectrodes are obtained by differentiating triangular voltage pulses in the coupling capacitors to the inputs of the "measure" and "reference" amplifiers. The insert is a schematic representation of the outputs from the two negative-capacitance amplifiers and from the difference amplifier before, during, and after impalement of a cell, with the lowest curve depicting the movement of the microelectrode

the high voltage pulse to the bender elements and a high degree of stiffness, so that the limiting factor for the precision of advancement of the electrode tip resided mainly in the electrode itself. The movement of the microelectrode with a pulse of 400 V across the bender elements was 20 to 25  $\mu$  in less than 1 msec. For the present study, the axial movements of the electrode were monitored with a capacitance transducer connected to a FM reactance converter (DISA, Copenhagen, Denmark, Model 51E01). The output from the reactance converter was displayed on the oscilloscope together with the signal from the microelectrode. When a high voltage pulse of the desired form was applied to the piezoelectric bender elements, the microelectrode was either moved directly into the cell, or retracted and then moved into the cell.

Measurement of the increment in resistance seen by the microelectrode tip after penetration into the cell was performed by passing intermittent diphasic constant-current pulses through the measuring microelectrode. The constant-current pulses were obtained by quasi-differentiation of triangular voltage pulses as described by Lettvin, Howland and Gesteland [16]. The resulting two diphasic voltage pulses were subtracted in a difference amplifier. The diphasic pulse from the reference electrode was adjusted to have the same waveform and magnitude as the pulse from the measuring microelectrode placed in the extracellular medium. In this bridge arrangement a resistance increase seen by the measuring electrode is indicated as a series of diphasic voltage pulses proportional in size to the increase in resistance. Changes in the d--c level of the measuring microelectrode tip appear on the oscilloscope as displacements of the whole trace including the diphasic pulses. Fig. 1 shows a schematic representation of tracings from the measuring electrode, the reference electrode and the output from the difference amplifier before, during and after impalement of a cell.

Capacitance neutralization amplifiers with input field effect transistors were used for the measuring and reference channels (Bioelectric Instruments, Farmingdale, New York, Model NF 1). These amplifiers were checked to have leak currents below  $10^{-12}$  A and input resistances above  $10^{11}$   $\Omega$ . When optimally neutralized, the time constant of the input with a typical microelectrode in the extracellular fluid was about 50  $\mu$ sec. This value is of importance for the evaluation of results with fast changing potential recordings.

The microelectrodes were drawn on a modified commercial microelectrode puller (Palmer, London, England), using Jena glass tubing with outer diameters of from 1.75 to 1.85 mm. The tips were checked regularly and after each adjustment of the pulling machine. For this purpose the tips were mounted in special rings, coated with approximately 100  $\text{\AA}$  of gold to avoid corona formation and observed in an electron microscope. The outer diameters of the tips were in the range of 0.17 to 0.20  $\mu$ . The tapering angle was below 5 degrees. The microelectrodes were filled with 3 M KCl from the back after initial submersion as described by Lassen and Sten-Knudsen [15]. The resistances were in the range of 8 to 20 M $\Omega$  when measured in Ringer's solution and the tip potentials were less than 3 mV (positive or negative). The microelectrodes were connected with the input cables via Ag-AgCl rods.

The cells for microelectrode measurements were prepared by diluting cell suspensions with Ringer's solution (37  $^{\circ}$ C) to give a final cytocrit of about 0.1%. This gave an appropriate number of cells on the bottom of the chamber. Furthermore, with this low cell volume fraction, the extracellular ion concentrations remained constant even under conditions where the cellular ion contents changed. Methylcellulose (0.5 to 1.0%) was added to the medium in order to reduce the tendency of the spherical cells to bounce away on introduction of the microelectrode.

## Results

The cellular concentrations of Na, K, and Cl are shown in Table 2 together with the calculated equilibrium potentials for chloride ions in sodium Ringer's and in potassium Ringer's. While the cell volume in sodium Ringer's was relatively stable, the cells in potassium Ringer's slowly swelled during the measurements. The values in sodium Ringer's are essentially in agreement with the findings of other investigators [6, 7, 8, 14, 18].

Table 2. Concentrations of sodium, potassium, and chloride in cell water, and calculated equilibrium potential for chloride ( $E_{Cl}$ )

Incubation medium	Na <sup>+</sup> (mEquiv/ liter)	K <sup>+</sup> (mEquiv/ liter)	Cl <sup>-</sup> (mEquiv/ liter)	$E_{Cl}$ <sup>a</sup> (mV)
Sodium Ringer's	46 ± 25	147 ± 26	58 ± 6	-26 (-20 to -29)
Potassium Ringer's <sup>b</sup>	7 ± 2	175 ± 8	119 ± 7	-7 (-4 to -9)

The values in Table 2 are given as mean ± one sd. The concentrations are corrected for dry matter in the cells. Dry to wet weight ratio in sodium Ringer's was  $0.24 \pm 0.04$ , and in potassium Ringer's ranged between 0.15 and 0.10.

<sup>a</sup>  $E_{Cl}$  is calculated from the chloride concentrations in this Table and Table 1. Furthermore,  $E_{Cl}$  was calculated in the individual experiments, and the values in parentheses give the range of  $E_{Cl}$  from 15 experiments in sodium Ringer's, and three experiments in potassium Ringer's, respectively.

<sup>b</sup> Mean values are given for cells incubated for 15 to 80 min in potassium Ringer's.

As mentioned in the Introduction, potential recordings from microelectrode measurements in this study fell in to two groups: stable potentials of about 8 mV, and transient potential recordings with peak values of 20 to 40 mV (inside negative in both cases). To follow the development of the experiments, the stable recordings will be considered first.

An example of a potential recording obtained from the puncture of a cell in sodium Ringer's is shown in Fig. 2. The bottom trace is the output from the transducer following the axial movements of the microelectrode. In this experiment, the microelectrode tip was pressed against the cell before releasing the rapid movement of the electrode by the piezoelectric driver. Due to contact with the cell, the resistance seen by the measuring electrode is increased and the potential is slightly positive. The forward movement of the microelectrode is preceded by a small retraction during which the resistance and potential changes are reduced. The retraction allowed the impact of the electrode tip with the cell membrane to occur at the highest obtainable speed. "Zero level" for potential and resistance can be seen in the right part of the trace, after the final retraction of the microelectrode. As the microelectrode is propelled forward, there is a potential drop to about -10 mV. This is given by the position of the dense line between the individual resistance measuring pulses. Simultaneously, the resistance rises to about 12 MΩ above the extracellular value. Upon retraction of the electrode, the potential and the resistance, as well as observation in the microscope, indicate that the electrode tip is back in the extracellular medium. In most cases the cells did not visibly change after

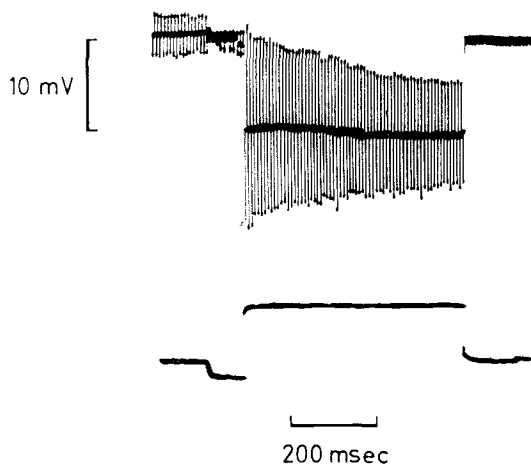


Fig. 2. Microelectrode measurement of an Ehrlich ascites cell in sodium Ringer's. The upper trace shows the potential variations before, during, and after impalement of a cell. The movement of the microelectrode is shown in the lower trace with forward movement depicted as an upward displacement of the trace. The total movement (not calibrated) was about  $20 \mu$ . The vertical calibration mark (10 mV) refers to the potential of the microelectrode. The horizontal time mark is common for both traces. The diphasic pulses for resistance measurement are calibrated so that a swing of 10 mV in each direction from the immediate d-c level corresponds to a resistance increase of  $10 M\Omega$ . It may be noted that the resistance was increased as the electrode was pressed against the cell before the impalement. The resistance change is decreased during the short initial retraction of the electrode

having been impaled. Occasionally, they became pale with a transparent vesicle forming on the cell surface at the site of impalement similar to the appearance shown by Schell and Neuhoff [20]. Usually, repetitive punctures on the same cell gave the same stable potential values until the cell finally changed appearance as described. The movement by the piezoelectric transducer of the microelectrode in cell-free Ringer's solution never gave changes in potential or resistance.

Fig. 3 shows the summary of more than a thousand measurements of the type demonstrated in Fig. 2. The mean value of the negative potentials is  $-8.1 \pm 2.2$  mV.<sup>2</sup> Positive potentials were obtained when the cell was only touched by the electrode, but, according to the impression of the observer, not penetrated. The mean of the positive potentials was 2.4 mV. The potential of  $-8.1$  mV was 3 mV less negative than the potential found by several other investigators (*see* Table 3) and thus even farther from the calculated Nernst potential for chloride, which in the present series of experiments ranged from  $-20$  to  $-29$  mV (*see* Table 2).

<sup>2</sup> Mean values are indicated  $\pm$  one SD.

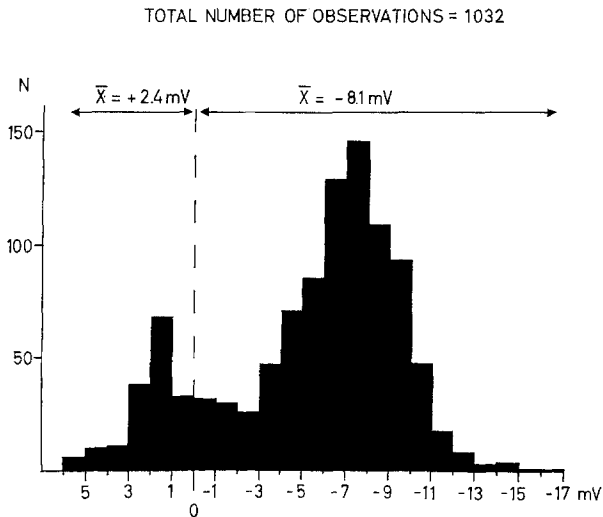


Fig. 3. Histogram of 1032 measurements on Ehrlich ascites cells in sodium Ringer's using a technique similar to that shown in Fig. 2. The abscissa shows the stable potential value, the ordinate ( $N$ ) gives the total number in each group of one mV. The mean values of the negative and positive potentials are indicated in the figure. A negligible number of measurements more negative than  $-17$  mV are omitted from the figure

Table 3. *Intracellular potential of Ehrlich ascites cells in sodium Ringer's*

Author	Potential <sup>a</sup> (mV)
Aull [1]	$-11.2 \pm 0.3$
Bernhardt and Pauly [3]	$-11.5 \pm 0.6$
Hempling [9]	$-11.1 \pm 2.8$
Johnstone [13]	$-20$ to $-40$
Sekiya [21]	$-8.6$ or $-16.9^b$

<sup>a</sup> The values are indicated as mean  $\pm$  one SEM.

<sup>b</sup> See text for further explanation.

At this point it was considered whether the cells were leaking as a consequence of the micropuncture. If this was the case, two questions immediately arose: (1) Is it possible to measure the true membrane potential before it is changed by eventual leaks?; and (2) What is the nature of the reproducibly measured potential of about  $-8$  mV?

To record potentials immediately after impalement of the cell, an oscilloscope with two time base generators and two dual trace differential amplifiers was used. The separate time bases were set at 0.5 and 20 msec/cm. In this way, both the fast response and the stable potential value in the same



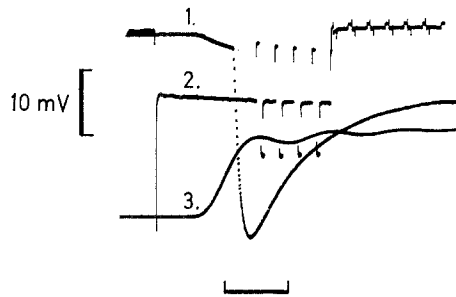


Fig. 4. Typical decaying potential obtained upon impalement of an Ehrlich ascites cell in sodium Ringer's. Trace 1 and trace 3 show the immediate events upon impalement. The horizontal time mark equals 1 msec for these two traces. Trace 1 is the potential seen by the microelectrode. Trace 3 follows the advancement of the microelectrode (total advancement about  $25 \mu$ ). Trace 2 shows the potential of the microelectrode but with a timebase 40 times slower than traces 1 and 3 (horizontal time mark equals 40 msec). The vertical calibration mark (10 mV) is common for the traces 1 and 2. The train of diphasic pulses for resistance measurement was started about 50 msec after the advancement of the microelectrode

cell could be recorded. By appropriate delay circuits, the two sweeps were placed suitably on the oscilloscope screen. Furthermore, the train of resistance measuring pulses was delayed until completion of the fast sweep. The movement of the microelectrode in immediate relation to the impalement was monitored on the second channel of the dual trace amplifier recording the fast potential response. A relatively large advancement step without retraction was used in the following experiments. Fig. 4 shows the result of a typical experiment with impalement of a cell in sodium Ringer's. Trace 1 is the potential measured by the microelectrode as seen at the fast sweep, trace 2 shows the output from a similar amplifier but with a sweep that moved 40 times slower. At the time when the electrode breaks through the cell membrane (sharp decline of trace 1), the potential drops to  $-30$  mV and climbs back in less than 5 msec to  $-10$  mV which is the potential level maintained during the slow sweep (trace 2). The resistance seen by the electrode tip is  $7.5 \text{ M}\Omega$  as indicated by the magnitude of the diphasic swings in trace 2. At retraction of the electrode, the potential and resistance values go back to their pre-puncture levels. Trace 3 shows that the microelectrode is driven forward within 0.5 to 0.7 msec. The slight oscillations in the position after the forward movement are due to the inherent mechanical properties of the piezoelectric driver (resonant frequency close to 1 kHz). The fast decaying negative potentials were reproducible

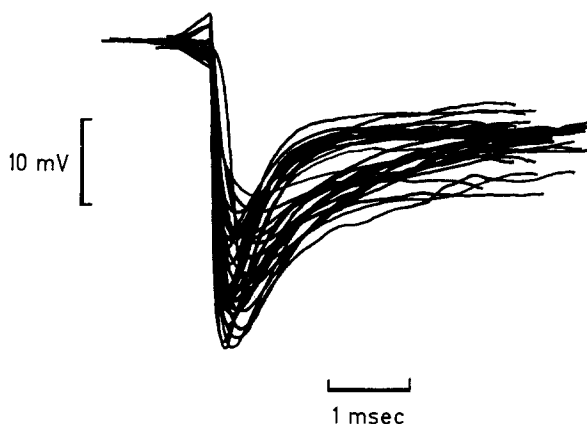


Fig. 5. Graphical superposition of 30 potential recordings obtained immediately after impalement of Ehrlich ascites cells in sodium Ringer's. The mean of the peaks was  $-26.5 \pm 5.0$  mV. The stable potentials in this group had a mean of  $-9.2 \pm 2.1$  mV. The mean time constant for the decay to a stable value was 0.8 msec

in sodium Ringer's. Fig. 5 shows the graphical superposition of 30 punctures on 30 different cells. The mean peak value of the potential was  $-26.5 \pm 5.0$  mV, and the mean of the stable potentials was  $-9.2 \pm 2.1$  mV. The peak value was reached after  $0.33 \pm 0.14$  msec. The decay towards the stable value followed a nearly exponential time course with a mean time constant of 0.8 msec.

Fig. 6 shows the summary of 549 peak values for potential recordings in sodium Ringer's. The histogram is cut off at values less negative than  $-13$  mV to ensure that the peak value recorded was more than twice the standard deviation different from the mean of the stable potentials. The mean of the peak potential values is  $-23.5 \pm 6.5$  mV. (In the calculation of the standard deviation, no correction was made for the distribution being non-Gaussian.)

As previously mentioned, repeated puncture of the same cell in most cases gave identical values for the stable potential. This is in contrast to the magnitude of the transients which became markedly smaller or vanished upon re-puncture (Fig. 7). In many cases, however, a second peak of similar magnitude as the first could be obtained if several min were allowed to elapse between the two punctures and provided that the cell was not visibly deteriorated.

A change of the suspending medium from sodium Ringer's to potassium Ringer's would be expected to depolarize the membrane as demonstrated

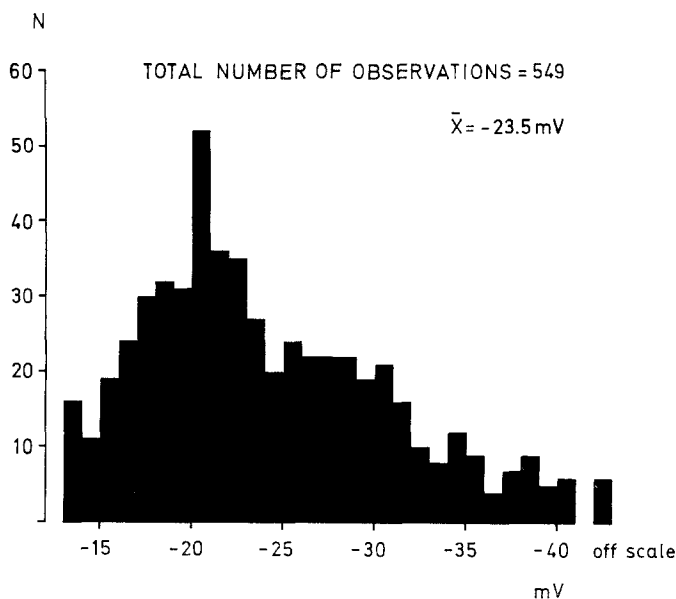


Fig. 6. Histogram showing the distribution of peak potentials obtained after impalement of Ehrlich ascites cells in sodium Ringer's. The graph is cut off at  $-13 \text{ mV}$  for reasons discussed in the text. The material is taken as the negative "peak" from recordings similar to those in Figs. 4 and 5. A few values marked "off scale" were too large to be recorded. The ordinate ( $N$ ) is the number of observations in each group of one mV. The abscissa is the potential in mV

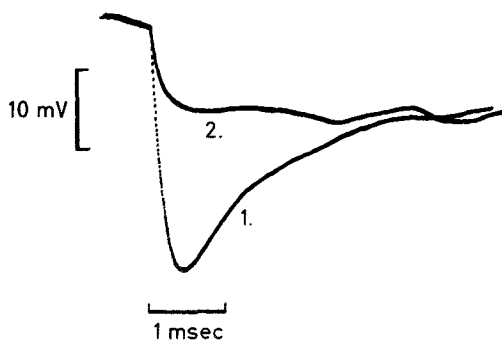


Fig. 7. Comparison of potentials recorded during first (1) and second (2) impalement of the same Ehrlich cell in sodium Ringer's. Experimental data as in Fig. 4

in numerous other tissues. In the present study the mean value of the stable potentials changed only from  $-8.1 \text{ mV}$  to  $-6.6 \pm 2.2 \text{ mV}$  when employing potassium Ringer's instead of sodium Ringer's. In striking contrast to this, the rapidly decaying negative potentials were abolished after about 15-min

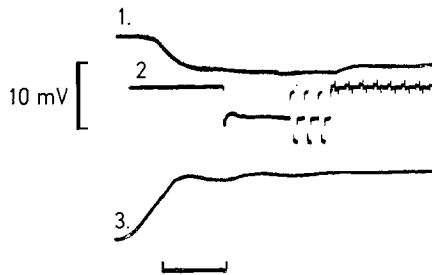


Fig. 8. Potential recording upon impalement of an Ehrlich ascites cell in potassium Ringer's. Traces 1 and 2 show the potential of the microelectrode and trace 3 follows the movement of the electrode. Calibrations and other data as in Fig. 4; the horizontal time mark indicates 1 msec (traces 1 and 3) and 40 msec (trace 2), respectively

incubation in potassium Ringer's as seen in Fig. 8. When cells, having been suspended in potassium Ringer's, were transferred back to sodium Ringer's, negative transient potentials could again immediately be recorded. These potentials were equal to, or larger than, those observed before suspension in potassium Ringer's.

In accordance with the findings of Maizels, Remington and Truscoe [17] we have found little effect of ouabain on the distribution ratio for chloride even with concentrations of ouabain giving a marked gain of cell sodium and loss of cell potassium. The chloride concentration in cells incubated in sodium Ringer's with 0.5 mM ouabain for 15 to 80 min was  $67 \pm 3$  mEq/liter of cell water. This corresponds to an  $E_{Cl}$  of  $-21.5$  mV. The mean of 96 peak values of potential recordings obtained under similar experimental conditions was  $-18.7 \pm 5.2$  mV. This value is not significantly different from the mode of the potentials shown in Fig. 6.

Other media and inhibitors of metabolism have been employed to compare the chloride distribution with the potential across the cell membrane. However, apart from the above reported experiments, the potential measurements were unsuccessful in the sense that the cells were either extremely fragile or shrunken. Under such conditions the cells appeared sticky and it was not possible to obtain reproducible potential measurements.

The resistance increase of the measuring electrode during impalement of the cells was recorded as previously described. This increase was  $8.0 \pm 4.3$  M $\Omega$  in sodium Ringer's and  $6.2 \pm 3.8$  M $\Omega$  in potassium Ringer's. The method employed was not fast enough to allow resistance measurements during the few msec in which the potential usually decayed to the stable value. All resistance measurements were thus made in a period with stable

potentials of the magnitude given in Fig. 3. No correlation was found between the magnitudes of resistance and potential changes in the individual experiments.

The influx of  $^{36}\text{Cl}$  into the Ehrlich cells in sodium Ringer's at  $38^\circ\text{C}$  was followed in six experiments. The influx followed an exponential course with a time constant of cellular chloride exchange of  $2.2 \pm 0.7$  min, consistent with the results of other investigators (Aull [1], Grobecker, Kromphardt, Mariani & Heinz [6], Kromphardt [14]). Using deproteinized samples, the cell chloride was found to be completely exchangeable with  $^{36}\text{Cl}$  [23].

### Discussion

If chloride ions are in electrochemical equilibrium in Ehrlich ascites cells as generally assumed [1, 6, 14, 23], the calculated equilibrium potential for chloride should equal the measured membrane potential. The Nernst potential for chloride can only be calculated if the intracellular and extracellular concentrations and activity coefficients are known. It has been reported that about 30 to 40% of the cell chloride does not exchange with added  $^{36}\text{Cl}$  [1, 14]. As shown by Simonsen and Nielsen [23], this apparent non-exchangeable fraction is an experimental artifact, and the cell chloride exchanges totally with the extracellular chloride. As there is no simple way for determination of the activity coefficients for ions in the high-protein intracellular fluid, it is assumed that the activity coefficients for chloride in the extracellular and intracellular fluids of these cells are equal.

In a number of experiments the calculated equilibrium potential for chloride in sodium Ringer's ranged between  $-20$  mV and  $-29$  mV (Table 2). Most previous microelectrode measurements of the membrane potential of the Ehrlich ascites cell are less negative than this value (Table 3). The most frequently obtained potential is about  $-11$  mV. The  $-11$  mV appears to correspond to the stable potential of  $-8$  mV observed in this study. The stable potential recordings in this study, thus, are even farther from the calculated equilibrium potential for chloride in earlier reports [1, 14, 23]. The peak recordings, however, are close to the Nernst potential for chloride and presumably closely related to the membrane potential proper.

When ascites cells are transferred to a high potassium Ringer's, the cell sodium and cell potassium approach steady state at concentrations close to the extracellular values. This means that the membrane potential under these conditions should be determined only by the Donnan potential. In potassium Ringer's a potential of  $-6.6$  mV was recorded immediately

after the penetration and remained constant during the impalement. This potential was identical to the chloride equilibrium potential. Upon retransferring the cells to sodium Ringer's, the peak potential recordings again showed the large negative potentials ( $-24$  mV) decaying to the usual stable value of about  $-8$  mV. Also in ouabain-containing medium the peak potential was close to the  $E_{Cl}$ . These findings can all be explained by assuming that the potential recorded immediately after penetration represents the membrane potential. It is unlikely that the transient potentials are caused by simple electrokinetic phenomena. Using the piezoelectric driver to move the electrode in Ringer's solution or in a homogenate of packed cells did not give rise to significant potential changes. As mentioned earlier, repeated puncture of the same cell led to decreasing or vanishing transient negative potentials with unchanged stable potentials.

The potentials measured by impalement of Ehrlich cells typically decayed in a few msec to a value of about  $-8$  mV. After the initial discharge, the value was essentially unaltered for several hundred msec. Potentials in this range could be obtained by repeated re-puncture even when the cell became shaggy and often with a bleb protruding at the site of the impalements. The stable potential was not much influenced by the ionic composition of the suspending medium, changing from  $-8.1$  mV in sodium Ringer's to  $-6.6$  mV in potassium Ringer's. This is in accordance with the potentials measured in the two media by Aull [1].

To elucidate the nature of the stable potential, cell concentrates were mechanically disrupted in a cooled, piston type homogenizer. The highly viscous homogenate was then placed in one end of the chamber used for measurements on intact cells and the remainder of the chamber was filled with Ringer's solution. The potential change was recorded as a microelectrode was moved from the Ringer's solution into the homogenate, and back into the Ringer's solution. The recorded potential change with sodium Ringer's was  $-5.9 \pm 1.0$  mV, with potassium Ringer's,  $-2.6 \pm 0.5$  mV, and with isotonic  $K_2SO_4$ ,  $+5.4 \pm 0.5$  mV. The values in sodium and potassium Ringer's are only slightly different from the stable potentials obtained by impalement of the cells in these two media. The value in isotonic  $K_2SO_4$  corresponds to the positive "membrane potentials" reported by Aull [1] in cells suspended in  $K_2SO_4$  medium. Since the stable potentials are not dependent on the presence of the intact cell membrane, it is likely that they are junction (diffusion) potentials between damaged cells and the medium.

Johnstone [13] reported stable intracellular potentials in the range of  $-20$  to  $-40$  mV. These values are in accordance with the rapidly measured

potentials in the present study, but the lack of detailed information in Johnstone's report excludes a further comparison. Sekiya [21] used a similar technique and described an initial potential drop after impalement to  $-8.6$  mV. Leaving the electrode in the cell, the potential declined to a minimal value of  $-16.9$  mV within 2 sec and then slowly drifted back either to a potential close to  $-8$  mV or to zero. This time sequence was interpreted as a sealing of the cell wall around the electrode at the time of the most negative potential followed by a gradual deterioration of the cell. Omitting retraction of the electrode, we were able to record a slow increase in negativity, similar to that reported by Sekiya [21], but the potential never became as negative as the initial potential drop. The intracellular potential of  $-16.9$  mV obtained by Sekiya [21] is about 8 mV less negative than the peak potentials in this study. The relatively large negative potentials obtained by Johnstone [13] and Sekiya [21] do not seem to be connected to the embedding of the cells in agar, in view of the fact that Hempling [9] and Bernhardt and Pauly [3] reported membrane potentials of  $-11$  mV with a similar technique.

Aull [1] used a pen recorder to follow the potential changes upon impalement of Ehrlich cells. The mean value of  $-11.2$  mV, reported as being the membrane potential, is calculated from the peak values obtained in each penetration. The only stable potential recording shown is about  $-9$  mV. It is likely that the value of the peaks was limited by the response time of the recorder (0.28 sec) which was three orders of magnitude slower than the measuring system used in the present study. The slow decay after the initial peak as seen by Aull may be related to complete deterioration of the cells.

The negative potentials obtained by Hempling [9], Aull [1] and Bernhardt and Pauly [3] are slightly more negative than the stable potentials reported here. The reason for this may be that the present study excluded all non-stable values for the calculation of the stable potential. As the non-stable potentials generally are more negative, they would bias the mean in a negative direction. In HeLa cells, Borle and Loveday [4] reported membrane potentials of  $-17$  mV and in KB cells, potentials of  $-13$  mV were obtained by Redmann, Stolte and Lüders [19]. In granulocytes, Beckmann, Jansen, Kalkoff and Redmann [2] found a stable intracellular potential of about  $-5$  mV. These potentials might be comparable to the stable potentials in this study. Concerning the potentials above zero obtained in sodium Ringer's in the present study, as well as by Aull [1], Johnstone [13], and Sekiya [21], it is our experience that the positive recordings are found when a cell wall is touched but not penetrated. Positive

potentials immediately prior to penetration of the cell membrane of fat cells were found by Girardier, Seydoux and Clausen [5].

The recorded peak potential after penetration of the cell membrane must be numerically smaller than the actual membrane potential of the unperturbed cell. The membrane potential decays from the peak value to the stable value with a time constant of about 1 msec. The potential variations were followed with a recording microelectrode and an amplifier with a short, but significant, composite time constant. In order to estimate the time course of recordings with various time constants of the electrode-amplifier system, the following simplifying equations were derived:

$$P = E_i \{1 - \exp(-t/\tau_1)\}, \quad (2)$$

and

$$E_i = (E_i^0 - E_s) \exp(-t/\tau_2) + E_s, \quad (3)$$

where  $P$  is the recorded potential,  $E_i$  is the intracellular potential at time  $t$ ,  $E_i^0$  is the membrane potential of the non-perturbed cell and  $E_s$  is the stable potential.  $\tau_1$  and  $\tau_2$  are the time constants for the recording system and the discharge of the membrane potential, respectively.

Inserting Eq. (3) into Eq. (2) gives:

$$P = \{(E_i^0 - E_s) \exp(-t/\tau_2) + E_s\} \{1 - \exp(-t/\tau_1)\}. \quad (4)$$

With  $\tau_1 = 80 \mu\text{sec}$  as a reasonable maximal figure for the time constant of the recording system, and  $\tau_2 = 800 \mu\text{sec}$ ,  $E_s = -9.2 \text{ mV}$  (*cf.* Fig. 5),  $E_i^0$  must take the value of  $-34 \text{ mV}$  to obtain a peak potential of  $-26.5 \text{ mV}$  (*cf.* Fig. 5). With this value, the time course of the recorded potential ( $P$ ) was computed from Eq. (4) (Fig. 9, curve "80"). Fig. 9 also shows the influence of different time constants of the recording system ( $\tau_1$ ), with the other parameters in Eq. (4) constant. It should be noted that the general pattern of the curves in Fig. 5 is similar to the computed curves.

The apparent large error of the peak potential as a measure of the membrane potential ( $E_i^0$ ) may be overestimated in this simple model. Usually the microelectrode was still in forward motion during the sharp potential drop prior to the peak (*see* Fig. 4). This would tend to reduce the leak as the wedge-shaped electrode is forced into the hole in the cell membrane. The electrical equivalent would be a large  $\tau_2$  in the first tenths of a msec and thus a numerically smaller  $E_i^0$ . Thus, Fig. 9 does not necessarily give the right magnitude of the error of the peak potential with regard to the true intracellular potential, but it clearly emphasizes the importance of using a recording system that is fast in comparison to the time course of the discharge.



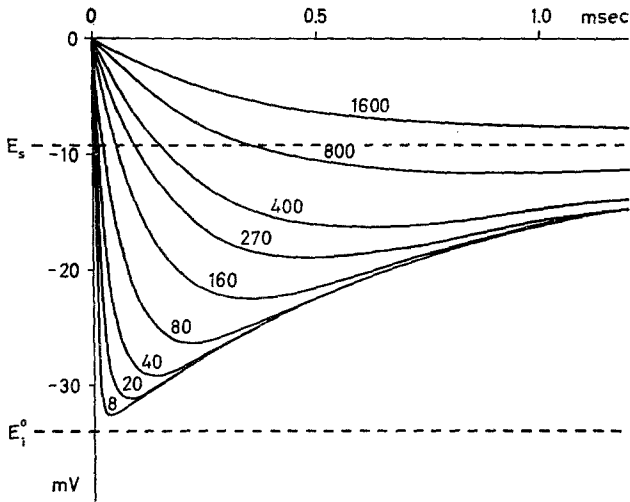


Fig. 9. A family of curves calculated from Eq. (4) for different time constants of the microelectrode-amplifier system ( $\tau_i$ ). These time constants (in  $\mu\text{sec}$ ) are indicated for each curve. The ordinate is the potential in mV. The abscissa is the time in msec.  $E_s$  is the stable potential ( $= -9.2$  mV) and  $E_i^0$  ( $= -34$  mV) is the calculated membrane potential of the unperturbed cell. The figure is discussed in detail in the text

The resistance increased by  $8\text{ M}\Omega$  when the electrode was moved into the cells. Part of this resistance increase (1 to  $2\text{ M}\Omega$ ) is to be expected as a result of the lower conductivity of the intracellular fluid. The remainder of the resistance increase (about  $7\text{ M}\Omega$ ) must be ascribed to characteristics of the cell membrane, possibly modified by a leak caused by the electrode. From the mean diameter of Ehrlich cells, Hempling [7] has calculated the surface area to be  $750\ \mu^2$ . From electron micrographs of Ehrlich ascites cells [10, 22] the presence of microvilli is estimated to increase the surface area by about 30%. Thus,  $1,000\ \mu^2$  is a reasonable value for the mean total cell surface. This leads to a specific membrane resistance of  $70\ \Omega\text{cm}^2$ .

The measured resistance of  $8\text{ M}\Omega$  can be compared to the total ionic conductance of the cell membrane from measurements of unidirectional tracer fluxes. Chloride permeates easily and is thus probably a main contributor to the membrane conductance. Using the expression derived for the equivalent resistance for an ion in equilibrium [11, 24], a "chloride resistance" for the membrane can be calculated:

$$R_{\text{Cl}} = (RT)/(F^2 M_{\text{Cl}}) \quad (5)$$

where  $R_{\text{Cl}}$  is the specific membrane resistance for chloride ions and  $M_{\text{Cl}}$  is the unidirectional flux for chloride.  $R$ ,  $T$  and  $F$  have their usual meanings.

Using the time constant for exchange of intracellular chloride of 2.2 min found in the present study, a mean cell volume of  $1,950 \mu^3$ , and a total cell surface of  $1,000 \mu^2$  including microvilli, the  $M_{Cl}$  is  $6.5 \times 10^{-11}$  moles  $\text{cm}^{-2} \text{sec}^{-1}$ . This gives a specific equivalent resistance of the cell membrane to chloride ions of  $4,000 \Omega \text{cm}^2$ . The chloride resistance for a cell with a total surface area of  $1,000 \mu^2$  is  $400 \text{ M}\Omega$ . This figure is about two orders of magnitude larger than the measured resistance. Eq. (5) is explicitly derived for an ion in equilibrium. During the passage of the diphasic current, the membrane potential is displaced, first in positive, then in negative direction. This means that chloride ions are not in equilibrium during the actual measurements of the resistance. Thus a direct comparison of the calculated and measured values of membrane resistance is not obviously permissible. Only the contribution of chloride ions to the membrane conductance has been considered. Other ions, especially sodium or potassium, may carry some of the current. These factors can not, however, explain a difference of two orders of magnitude. The relatively low resistance measured may thus be dominated by a leak in the cell membrane caused by the microelectrode.

Potential measurements on human red cells have been performed by Lassen and Sten-Knudsen [15] and by Jay and Burton [12]. These studies may, in principle, have suffered from leak problems similar to those encountered in the present work. The small size of the human red cell ( $160 \mu^2$ ) would cause a rapid discharge of the membrane potential through a leak around the electrode. Furthermore, as the junction potential between damaged red cells and plasma presumably is close to the membrane potential, eventual transients as described for the Ehrlich cell must be small. The procedure of impalement used by Jay and Burton [12] would not permit detection of transients.

Tupper and Tedeschi [25–27] have reported positive membrane potentials and low membrane resistances in measurements on mitochondria from *Drosophila*. In state 4 the potential was about  $+10 \text{ mV}$  (inside positive) and the resistance about  $2 \Omega \text{cm}^2$ . In state 3 the corresponding values were  $+19 \text{ mV}$  and  $4 \Omega \text{cm}^2$ . The very small size of the mitochondrion (surface area about  $40 \mu^2$ ) would make it difficult to measure a discharging membrane potential. Using Eq. (4) with a recording system time constant ( $\tau_1$ ) of  $80 \mu\text{sec}$  (shorter than the time constant estimated from the work of Tupper & Tedeschi),  $E_s = 10 \text{ mV}$ , and  $E_i^0$  of either  $20 \text{ mV}$  or  $-20 \text{ mV}$ , the expected time course for the recording is shown in Fig. 10. The discharge time constant ( $\tau_2$ ) is set to  $40 \mu\text{sec}$ , corresponding to the small surface area of the mitochondrion as compared to the Ehrlich cell. The resulting curves

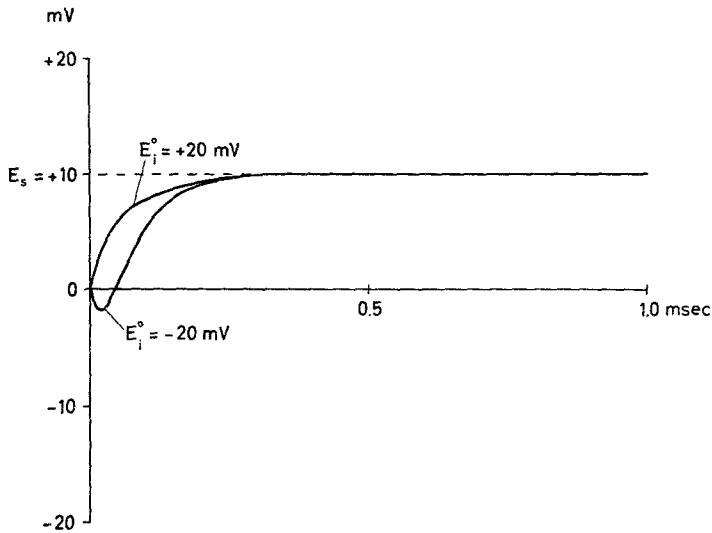


Fig. 10. Computed potential recordings as calculated from Eq. (4). The  $E_s$  (stable potential) and the time constants in Eq. (4) are chosen as relevant to studies on isolated mitochondria [25–27]. The effect on the recordings of setting  $E_i^0$  to either +20 mV or –20 mV is shown. The time course of the recorded potential is clearly dominated by the recording system

are, despite the chosen short  $\tau_1$ , dominated by the time constant of the electrode-amplifier system, and not by the intramitochondrial potential before the puncture (+20 mV or –20 mV in this example). Thus, it is difficult to evaluate whether the recordings represent membrane potentials or liquid junction potentials similar to the stable potentials in this study.

In conclusion, it should be emphasized that the use of microelectrodes for measurements on isolated cells or organelles in suspension calls for great care in the interpretation of the results.

Mr. Ole Bengtson is gratefully acknowledged for the computation on analogue models.

### References

1. Aull, F. 1967. Measurement of the electrical potential difference across the membrane of the Ehrlich mouse ascites tumor cell. *J. Cell. Physiol.* **69**:21.
2. Beckmann, A., Jenssen, H. L., Kalkoff, W., Redmann, K. 1970. Das bioelektrische Potential an der zytoplasmatischen Membran der Granulozyten. *Experientia* **26**:186.
3. Bernhardt, J., Pauly, H. 1967. Das Membranpotential von Ehrlich-Aszitestumorzellen. *Biophysik* **4**:101.
4. Borle, A. B., Loveday, J. 1968. Effects of temperature, potassium and calcium on the electrical potential difference in HeLa cells. *Cancer Res.* **28**:2401.

5. Girardier, L., Seydoux, J., Clausen, T. 1968. Membrane potential of brown adipose tissue. A suggested mechanism for the regulation of thermogenesis. *J. Gen. Physiol.* **52**:925.
6. Grobecker, H., Kromphardt, H., Mariani, H., Heinz, E. 1963. Untersuchungen über den Elektrolythaushalt der Ehrlich-Ascites-Tumorzelle. *Biochem. Z.* **337**:462.
7. Hempling, H. G. 1958. Potassium and sodium movements in the Ehrlich mouse ascites tumor cell. *J. Gen. Physiol.* **41**:565.
8. — 1959. Ion movements and the maintenance of tumor cell volume. *Fed. Proc. Fed. Amec. Soc. Exp. Biol.* **18**:67.
9. — 1962. Potassium transport in the Ehrlich mouse ascites tumor cell: Evidence for autoinhibition by external potassium. *J. Cell Comp. Physiol.* **60**:181.
10. Herdson, P. B., Kaltenbach, J. P. 1966. Fine structural changes in hypotonically treated Ehrlich ascites tumor cells. *Exp. Cell Res.* **42**:74.
11. Hodgkin, A. L., Keynes, R. D. 1955. The potassium permeability of a giant nerve fibre. *J. Physiol.* **128**:61.
12. Jay, A. W. L., Burton, A. C. 1969. Direct measurement of potential difference across the human red blood cell membrane. *Biophys. J.* **9**:115.
13. Johnstone, B. M. 1959. Micro-electrode penetration of ascites tumour cells. *Nature* **183**:411.
14. Kromphardt, H. 1968. Chloridtransport und Kationenpumpe in Ehrlich-Asciteszellen. *J. Biochem.* **3**:377.
15. Lassen, U. V., Sten-Knudsen, O. 1968. Direct measurements of membrane potential and membrane resistance of human red cells. *J. Physiol.* **195**:681.
16. Lettvin, J. Y., Howland, B., Gesteland, R. C. 1958. Footnotes on a head stage. *I.R.E. Trans. Med. Electron.* **10**:26.
17. Maizels, M., Remington, M., Truscoe, R. 1958. The effects of certain physical factors and of the cardiac glycosides on sodium transfer by mouse ascites tumour cells. *J. Physiol.* **140**:61.
18. — — — 1958. Metabolism and sodium transfer of mouse ascites tumour cells. *J. Physiol.* **140**:80.
19. Redmann, K., Stolte, C., Lüders, D. 1967. Membranpotential-Messungen an KB-Zellkulturen. *Naturwissenschaften* **54**:255.
20. Schell, P. L., Neuhoff, V. 1968. UV-Beobachtung an unfixierten Ehrlich-Ascites-Sarkom-Zellen. *Naturwissenschaften* **55**:496.
21. Sekiya, T. 1962. Studies on the membrane potential of Ehrlich ascites tumor cell. *Gann* **53**:41.
22. Selby, C. C., Biesele, J. J., Grey, C. E. 1956. Microscope studies of ascites tumor cells. *Ann. N.Y. Acad. Sci.* **63**:748.
23. Simonsen, L. O., Nielsen, A.-M. T. 1971. Exchangeability of chloride in Ehrlich ascites tumor cells. *Biochim. Biophys. Acta* **241**:522.
24. Tosteson, D. C. 1959. Halide transport in red blood cells. *Acta Physiol. Scand.* **46**:19.
25. Tupper, J. T., Tedeschi, H. 1969a. Microelectrode studies on the membrane properties of isolated mitochondria. *Proc. Nat. Acad. Sci.* **63**:370.
26. — — 1969b. Microelectrode studies on the membrane properties of isolated mitochondria. II: Absence of a metabolic dependence. *Proc. Nat. Acad. Sci.* **63**:713.
27. — — 1969c. Mitochondrial membrane potentials measured with microelectrodes: Probable ionic basis. *Science* **166**:1539.